Double-electron recombination in high-order-harmonic generation driven by spatially inhomogeneous fields

Alexis Chacón,[1] Marcelo F. Ciappina,[2,3] and Maciej Lewenstein[1,4]

[1]*ICFO-Institut de Ciències Fotòniques, The Barcelona Institute of Science and Technology, 08860 Castelldefels (Barcelona), Spain*

[2]*Max-Planck-Institut für Quantenoptik, Hans-Kopfermann-Strasse 1, D-85748 Garching, Germany*

[3]*Institute of Physics of the ASCR, ELI-Beamlines, Na Slovance 2, 182 21 Prague, Czech Republic*

[4]*ICREA-Institució Catalana de Recerca i Estudis Avançats, 08010 Barcelona, Spain*

(Received 7 November 2015; revised manuscript received 20 May 2016; published 7 October 2016)

We present theoretical studies of high-order harmonic generation (HHG) driven by plasmonic fields in *two-electron* atomic systems. Comparing the single- and two-electron active approximation models of the hydrogen negative ion, we provide strong evidence that a nonsequential double-electron recombination mechanism appears to be mainly responsible for the HHG cutoff extension. Our analysis is carried out by means of a reduced one-dimensional numerical integration of the two-electron time-dependent Schrödinger equation, and on investigations of the classical electron trajectories, resulting from the Newton's equation of motion. Additional comparisons between the hydrogen negative ion and the helium atom suggest that the double recombination process depends distinctly on the atomic target. Our research paves the way to the understanding of strong field processes in multielectronic systems driven by spatially inhomogeneous fields.

DOI: 10.1103/PhysRevA.94.043407

I. INTRODUCTION

The incessant development of ultrafast, femtosecond (10^{-15} s) laser technology in the infrared (IR) regime has opened new avenues to study a wide range of strong field laser-matter processes at their natural time scale [1–3]. These invaluable experimental and technological tools have allowed physicists to address instrumental aspects of one of the most fundamental processes: the tunneling ionization of atoms and molecules [3]. In particular, the application of this laser technology has provided a key factor for the understanding of the main mechanisms underlying the emission of coherent radiation from atoms or molecules [2,4–6].

As a matter of fact, one could say the high-order harmonic generation (HHG) process fits within the tunneling ionization regime, when the Keldysh parameter, defined by $\gamma = \sqrt{\frac{I_p}{2U_p}}$, is $\gamma \leqslant 1$. I_p and $U_p = \frac{\mathcal{E}_0^2}{4\omega_0^2}$ denote here the ionization potential of the atomic or molecular target and the electron ponderomotive potential energy in atomic units, respectively. $\mathcal{E}_0$ is the peak amplitude of the laser electric field and ω_0 the carrier frequency. The so-called three-step or "simple man's" picture describes the underlying physics behind the HHG phenomenon [5]. In the first step, occurring about the maximum of the strong laser electric field, the Coulomb potential is deformed in such a way that a potential barrier is formed. Then, the electron is able to tunnel out throughout this "atomic barrier", and the atom is then ionized. In the second step, or better to say phase, once the electron is in the continuum, the electric field of the laser accelerates it. Naturally, the electron gains energy from this oscillating field, converting it into kinetic energy. Consequently, when the electric field changes its sign, the electron reverses the direction of its motion and has a certain probability to recombine back to the ground state of the remaining ion core. In this third step the electron excess energy is converted into an attosecond burst of coherent radiation, typically in the XUV spectral range. In particular, the maximum emitted harmonic order can be obtained using purely classical arguments and it has a value of $n = (I_p + 3.17U_p)/\omega_0$ [5,6].

One of the main challenges in the production of HHG driven by IR femtosecond laser fields is the requirement of extra laser cavities for increasing up the peak power of the oscillator output, given the fact that intensities of the order of 10^{13}–10^{14} W/cm^2 are needed for the HHG process to happen in atoms, typically noble gases. A step forward to mitigate this issue was proposed by Kim and co-workers [7]. By focusing a laser pulse of moderate intensity, about 10^{11} W/cm^2, coming directly from a femtosecond oscillator output, onto a bow-tie-shaped gold nanostructure array, an enhancement of about 20 dB of the laser peak intensity on each of the elements was obtained. When argon atomic gas was injected in the vicinity of each nanostructure, high-order harmonic emission of the fundamental frequency of the laser beam was observed [7].

One should stress, however, that the experimental outcomes of Kim's experiment are controversial. Nevertheless, they have stimulated persistent and promising theoretical activities. Several problems are attributed to such an experiment, namely, (i) the impossibility to disentangle the coherent from the incoherent radiation emission, i.e., to distinguish between HHG and atomic line emission (ALE), and issues related with the conversion efficiency (see, e.g., [8–10]); (ii) the unrealistic predictions related to the field enhancement (see, e.g., [11]); and (iii) the concrete feasibility to reach the damage intensity threshold of the materials, modifying substantially the geometry of the nanoemitters and consequently the amplification of the incoming laser field.

The pioneering theoretical works performed on HHG driven by plasmonic fields have confirmed two main facts, specifically: (i) an enhancement of the emitted harmonics signal, and (ii) a large extension in the harmonic cutoff. These two features are mainly due to the spatial variation at a nanometer scale of the laser electric field along the laser polarization axis (see, e.g., [12–16]).

Most of the approaches to model HHG, both driven by conventional and spatially inhomogeneous fields, are based on the hypothesis that a single active electron (SAE) approximation is good enough to describe the harmonic emission. Thereby, those pictures neglect electron-electron interactions in the atomic systems commonly used to produce high-order harmonics, such as He, Ar, Xe, etc. [4]. Nevertheless, studies of HHG considering two- and multi-electron effects have been performed by several authors [17–23]. From these contributions one could conclude that depending on the atomic target properties and the laser frequency and/or intensity regime, multielectron effects could play an important role in HHG [17–19]. For instance, Sanpera *et al.* have demonstrated that no electron-electron correlation effects were observed in the HHG driven at relative low intensity 4×10^{14} W/cm^2 in a one-dimensional (1D) helium model. On the contrary, theoretical studies carried out by Koval *et al.* have shown that a nonsequential double recombination (NSDR) mechanism is the responsible of the features observed in the HHG spectra at higher laser intensities [19]. Furthermore, an extension in the HHG cutoff and a clear interference structure was predicted in the hydrogen negative ion. Consequently, it was argued that single- and double-electron ionization processes play an important role for this particular two electron system [17,18].

We should mention, however, that all these theoretical approaches have been developed for spatially homogeneous fields, contrary to the studies of HHG in two-electron ($2e$) systems driven by spatially inhomogeneous field we report here.

In this article we propose plasmonic fields as a tool to study multielectron effects in HHG from $2e$ systems. We focus our investigations on the study of the $2e$ hydrogen negative ion (H^-) and the helium atom (He). By comparing the numerical solutions of a reduced 1D–time-dependent-Schrödinger equation (1D-TDSE) for both the two-active electron (TAE), and the SAE models, we can trace out the analogies and differences in the HHG process from these two atomic systems, *a priori* very similar in their intrinsic structure. The interpretation of our numerical results renders on a semiclassical approach based on the time-frequency analysis of the quantum outcomes, and the classical integration of Newton's equation of motion.

II. THEORY

In order to investigate whether double-electron ionization effects in the HHG spectrum driven by plasmonic fields exist, we model H^- and He by employing SAE and TAE approximations.

Since the dynamics of an atomic electron driven by a strong laser field, in the SAE approximation, is mainly along the direction of the laser electric field (in a linearly polarized laser pulse), it is reasonable to employ approaches based on a 1D spatial dimension.

In particular, these models have been extensive and successfully applied to describe strong field processes, e.g., HHG and above-threshold ionization (ATI), both in spatially homogeneous and inhomogeneous fields. For a review about the strong field process in spatially homogeneous fields, see, e.g., [24]; for the application of 1D models to HHG and ATI driven by spatially inhomogeneous fields, see, e.g., [13,15] and [25], respectively. On the other hand, for the TAE approach, each of the two electrons dynamics is restricted to a "1D line", i.e., we end up with a 1D × 1D scheme. The 1D models of both H^- and He are described in Refs. [18] and [17,26], respectively, and we shall thus present here only a brief summary.

The Hamiltonian H of our $2e$ systems can be written in the length gauge as

$$H = \frac{1}{2}\sum_{j=1}^{2}\left[p_j^2 + V(z_j)\right] + V_{ee}(z_1,z_2) + V_{\rm int}(t), \qquad (1)$$

where

$$V(z_j) = -\frac{Z}{\sqrt{z_j^2 + a}} \qquad (2)$$

and

$$V_{ee}(z_1,z_2) = \frac{1}{\sqrt{(z_1 - z_2)^2 + b}} \qquad (3)$$

are the jth nucleus-electron soft-core Coulomb attractive potential, and the electron-electron soft-core Coulomb repulsion interaction, respectively. Note that in Eq. (1)

$$V_{\rm int}(t) = \sum_{j=1}^{2} z_j\left(1 + \frac{\epsilon}{2}z_j\right)E_{\rm h}(t) \qquad (4)$$

defines the coupling of each of the two electrons with the plasmonic field, in the dipole approximation, for a linearly polarized laser field in the z axis. The parameter ϵ governs the inhomogeneity strength of the plasmonic field and represents a *caricature* of the actual plasmonic field [15]. This linear model, however, appears adequate to capture the dynamics of an electron moving in a spatially inhomogeneous field. Here, ϵ has units of inverse length (see e.g. [12,13]). In Eq. (4) $E_{\rm h}(t)$, is the *conventional* laser electric field defined according to

$$E_{\rm h}(t) = \mathcal{E}_0 f(t)\sin(\omega_0 t + \varphi_0), \qquad (5)$$

where $f(t)$ denotes the pulse envelope and φ_0 the carrier envelope phase (CEP).

Moreover, the one-electron Hamiltonian reads

$$H = \tfrac{1}{2}p^2 + V(z) + V_{\rm int}(t), \qquad (6)$$

where a short-range Pöschl-Teller potential (PTP) [27,28]

$$V(z) = -\frac{V_0}{2}\mu^2\,\mathrm{sech}^2(\mu z) \qquad (7)$$

is employed to model the outer electron of our H^- system and now

$$V_{\rm int}(t) = z\left(1 + \frac{\epsilon}{2}z\right)E_{\rm h}(t). \qquad (8)$$

In order to compute the two-electron ground state of H^-, we set $a = b = 1$ a.u. and $Z = 1$. The binding eigenenergy with these parameters is $E_0 = -0.73$ a.u. In our model for H^-, the I_p of the inner electron is $I_p^{(\rm i)} = 0.66$ a.u.; thereby the corresponding I_p of the outer electron will be about $I_p^{(\rm o)} \sim 0.1$ a.u. [18,29]. For the SAE approach, we choose in Eq. (7) $\mu = 1$ and $V_0 = 0.75$ a.u., to match the $I_p^{(\rm o)}$ of H^-. The numerical solution of the 1D-TDSE for the SAE and TAE models is performed using the split-spectral operator method [30–32].

First, by imaginary time-propagation with a time step of $\delta t = -0.03i$ a.u., we integrate the laser-free Schrödinger equation and obtain the ground state wave function. Once the initial state of the system is set, the emitted harmonic yield, or HHG spectrum, is computed by Fourier transforming the dipole acceleration $\langle a_d(t)\rangle$, i.e., $I_{\rm HHG}(\omega) = |\mathcal{F}[\langle a_d(t)\rangle]|^2$; for the TAE model it is thus mandatory to compute the $2e$ wave function $\Psi(z_1,z_2,t)$, while for the SAE model the one-electron wave function $\Psi(z,t)$ is sufficient. For this aim we numerically integrate the reduced 1D-TDSE for both models. In particular, in the case of the SAE approximation, only the outer electron is considered [17,18,33].

The $2e$ position grids have lengths of $L_1 = L_2 = 2500$ a.u., with steps of $\delta z_1 = \delta z_2 = 0.25$ a.u., respectively. The same grid parameters are used in case of the SAE approach, but only along a one-dimensional line. In the SAE model $\langle a_d(t)\rangle$ reads

$$\left\langle a_d^{\rm SAE}(t)\right\rangle = \langle\Psi|\frac{\partial V(z)}{\partial z}|\Psi\rangle; \tag{9}$$

meanwhile for the TAE scheme is

$$\left\langle a_d^{\rm TAE}(t)\right\rangle = \langle\Psi_{1,2}|\sum_{j=1}^{2}\frac{\partial}{\partial z_j}[V(z_j)+V(z_1,z_2)]|\Psi_{1,2}\rangle. \tag{10}$$

The emitted harmonic yields obtained within the TAE model is divided by a factor of 4, in order to take into account the two electrons of the corresponding atomic system. In this way a direct comparison with the SAE results can be made.

In addition to the quantum models, we have numerically solved the Newton's equation:

$$\dot{p}_z(t) = -[1+\epsilon z(t)]E_{\rm h}(t), \tag{11}$$

to compute the classical highest electron energy at recollision $E_{\rm max}$. We note that the spatially inhomogeneous electric field introduces substantial changes in the electron trajectory $z(t)$ (see, e.g., [13,16]). For conventional fields, i.e., when $\epsilon = 0$, this maximum energy at recollision is given by the usual expression $E_{\rm max} = 3.17U_p$ [5]. The classical calculation of $E_{\rm max}$ allows us to estimate the maximum harmonic order $n_1 = (I_p^{\rm (o)} + E_{\rm max})/\omega_0$ of the HHG process driven by the spatially inhomogeneous field. To distinguish between the conventional cutoff and the spatially inhomogeneous one, we shall denote them as n_1 and n_1', respectively.

III. RESULTS

A. Harmonic emission of two-electron systems driven by plasmonic fields

Figure 1 shows the HHG spectra of the H^- as a function of the inhomogeneity degree, governed by ϵ, for both the SAE [Fig. 1(a)] and TAE [Fig. 1(b)] models. Clearly, as ϵ increases, noticeable discrepancies in the harmonic emission structure and the cutoff are observed between the models. In case of the SAE approach depicted in Fig. 1(a), the classical cutoff n_1' is in very good agreement with the maximum energy of the emitted photon. On the contrary, for the TAE model, the classically predicted maximum harmonic order n_1' is unable to match the cutoff obtained quantum mechanically, even for the case of $\epsilon = 0$. Hence, we denote this "new" cutoff for the

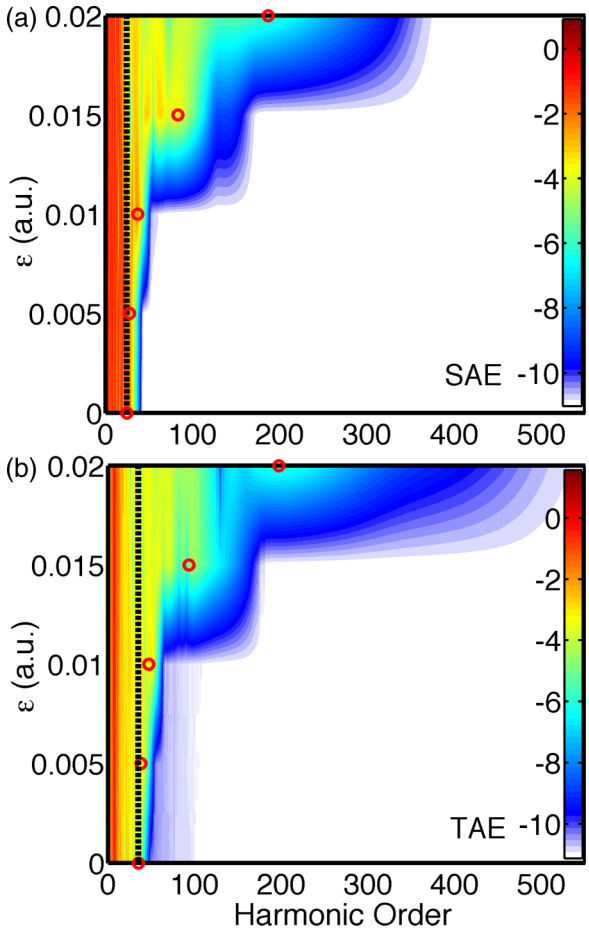

FIG. 1. HHG yield of H^- driven by a spatially inhomogeneous field for (a) the SAE and (b) the TAE approximations, respectively. The color scale is logarithmic and in arbitrary units. Black vertical dashed lines denote the cutoff for (a) the SAE conventional field n_1 and (b) the TAE n_2. Red circles are the calculated classical cutoffs as a function of ϵ according to our definition of n_1' and n_2' (see the text for more details). The IR laser pulse parameters are electric field strength $\mathcal{E}_0 = 0.0756$ a.u. (corresponding to a peak enhanced intensity of $I_0 = 2.0\times10^{14}$ W cm^{-2}), $\omega_0 = 0.057$ a.u. (photon energy 1.55 eV), $\varphi_0 = 0$ rad, and $f(t) = \sin^2(\frac{\omega_0 t}{2N})$ with three total cycles [the corresponding full width at half maximum (FWHM) is 2.6 fs].

H^- TAE model by n_2. Logically, a natural question arises: where does this clear disagreement between the SAE and TAE models come from? (Note that the disparity is clearly visible for both the conventional and spatially inhomogeneous electric field cases).

In order to address the above question, in Figs. 2(a) and 2(b) we compare the emitted HHG spectra for two specific cases: $\epsilon = 0$ and $\epsilon = 0.02$ a.u., respectively. On the one hand, for conventional fields and in the case of $2e$ systems, where double-electron ionization contributions are not relevant, one can expect that the cutoffs n_1 and n_2 coincide [17]. The results depicted in Fig. 2(a) clearly shows this is not the case: an extra extension in the $I_{\rm HHG}^{\rm (TAE)}(\omega)$ cutoff with respect to the SAE model, is found. According to Lappas *et al.* [17], possible inner-electron contributions to the harmonic spectrum should extend the cutoff by an extra amount

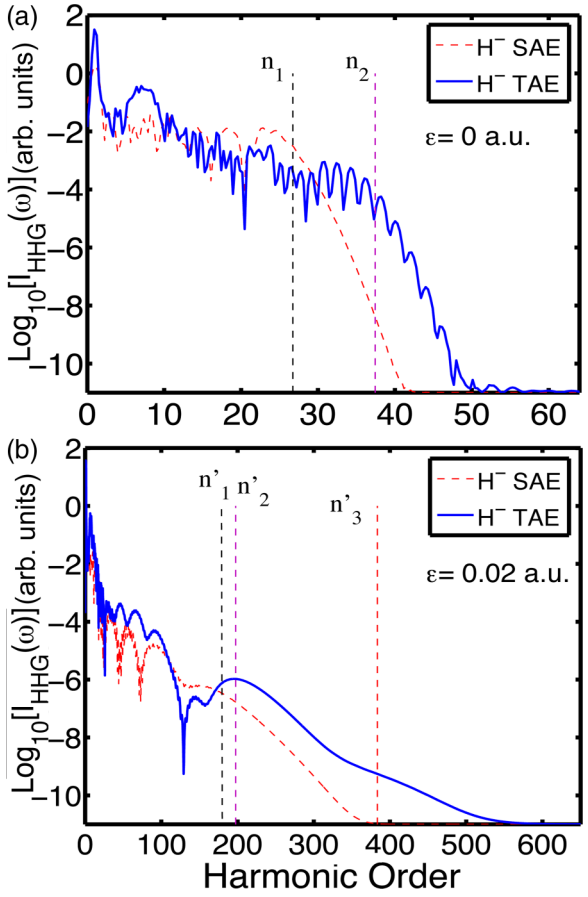

FIG. 2. (a) Conventional and (b) inhomogeneous emitted HHG spectra of H^- for our SAE and TAE models. In the HHG driven by a conventional field, the classical cutoff energy for the SAE and TAE calculations are denoted by n_1 (black vertical dashed line) and n_2 (violet vertical dashed line), respectively. The n_1', n_2', and n_3' (red vertical dashed line) denote the cutoff for the SAE, TAE, and the nonsequential double-electron recombination mechanism (see the text), respectively.

of $n_{\text{shift}} = (I_p^{(i)} - I_p^{(o)})/\omega_0$ [17–19]. Consequently, we could argue that the main mechanism behind this HHG extension is a *sequential double-electron recombination* of the outer and inner electrons. In this process both electrons are launched to the continuum at two consecutive electric field maxima and then, after about three-quarters of a laser cycle, both electrons *sequentially* recombine to their respective "ground states." This process leads to a cutoff given by $n_2 = n_1 + n_{\text{shift}}$ which is in reasonable agreement with the HHG spectrum computed by our TAE model.

On the other hand, Fig. 2(b) shows the emitted HHG spectra driven by a spatially inhomogeneous field for both the SAE and TAE models. First, and similarly to the conventional field case, a structural difference between the two models is observed in the HHG spectra, which comes from the different nature of the electron recombination events. Furthermore, the harmonic cutoff predicted by the SAE model is well reproduced by n_1'. Second, a large high harmonic "cutoff" appears in the case of the computed HHG by means of the TAE model. Such a "cutoff" cannot be explained by $n_2' = (E_{\max} + I_p^{(o)})/\omega_0 + n_{\text{shift}}$, where $E_{\max}$ denotes the maximum electron energy at the recollision time. This indicates that another *mechanism* should be responsible for this extension. One candidate to explain this increase could be a NSDR event [19].

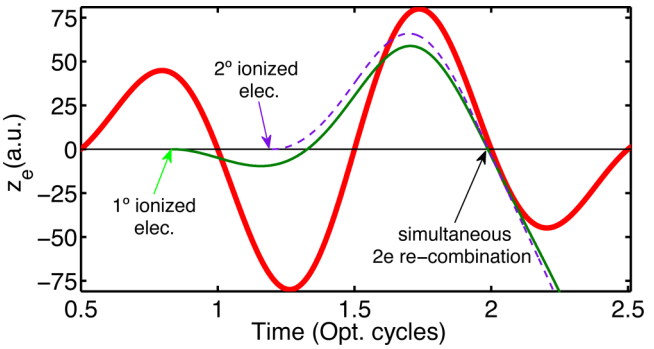

FIG. 3. Classical electron trajectory calculations for the nonsequential double-electron recombination mechanism driven by a plasmonic field. The green solid and violet dashed lines correspond to the most probable first and second ionized electron trajectories, respectively. The black arrow points out the simultaneous recollision (recombination) event. The red solid line denotes the time profile of the plasmonic electric field.

In order to probe this hypothesis, from classical calculations we can test if the inner and outer electrons will simultaneously recombine to their ground states with maximum energies $E_{\max}^{(1st)}$ and $E_{\max}^{(2nd)}$, respectively. The emitted harmonic order cutoff could then be obtained by [19]

$$n_3' = \left(E_{\max}^{(1st)} + E_{\max}^{(2nd)} + I_p^{(i)} + I_p^{(o)}\right)/\omega_0. \tag{12}$$

Figure 3 helps to classically describe this double NSDR process. The classical trajectories for the two electrons are obtained by integrating Eq. (11) with an inhomogeneity parameter $\epsilon = 0.02$ a.u. This picture assumes that both electrons are sequentially ionized via tunneling about the two consecutive laser field maxima. These ionization events are denoted by green and violet arrows, respectively. Then, the two electrons propagate into the continuum according to those trajectories depicted in green and violet lines. As it is clearly indicated by the black arrow in Fig. 3, these probable trajectories can simultaneously recollide with the parent ion. Both electrons, at this recollision time, carry excess energies $E_{\max}^{(1st)}$ and $E_{\max}^{(2nd)}$, respectively. Via this NSDR process, the excess energy is converted into a high XUV photon [see Eq. (12) for the actual computation of the energy limit]. Furthermore, in Fig. 2(b) we observe that the value of n_3' is in excellent agreement with our TAE model calculations. All the above mentioned arguments support the fact that the NSDR mechanism is responsible for this extra cutoff extension for the case of H^- (see the subsequent discussion for more details).

Pursuing to find a broader panorama about the behavior of $2e$ systems, we have computed the HHG spectra of the He atom for both conventional and spatially inhomogeneous fields. The same SAE and TAE models of He described in [17,26] have been implemented. Similarly to the H^-, for the SAE approach we have integrated in a 1D-TDSE the outer electron of He. In such a case, the long-range soft-core Coulomb potential described in [17] is used to obtain an $I_p^{(o)} = 0.73$ a.u. The

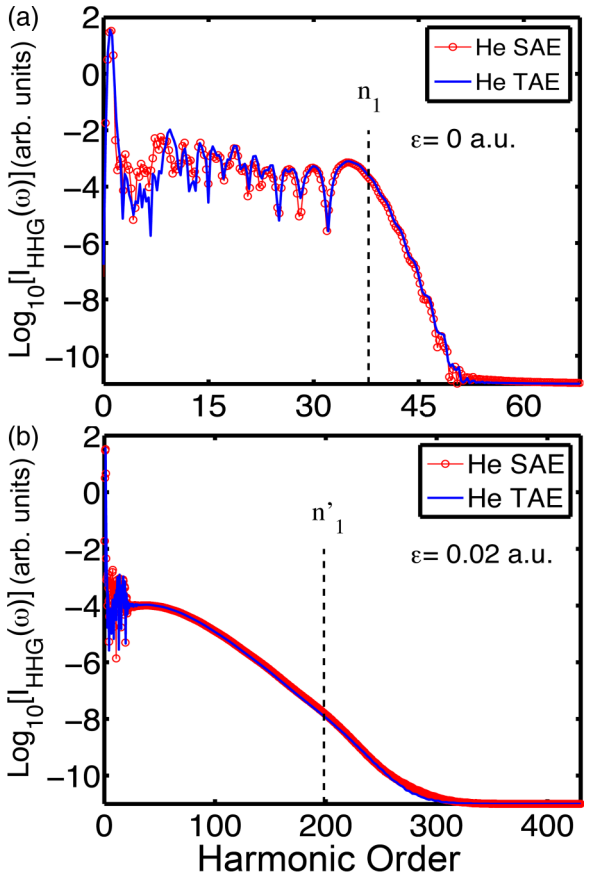

FIG. 4. HHG for the He atom. The HHG spectra of (a) and (b) are computed with the same laser parameters as in Fig. 2. Black dashed vertical lines denote (a) the n_1 conventional field cutoff for the outer electron, and (b) n_1' the inhomogeneous field cutoff.

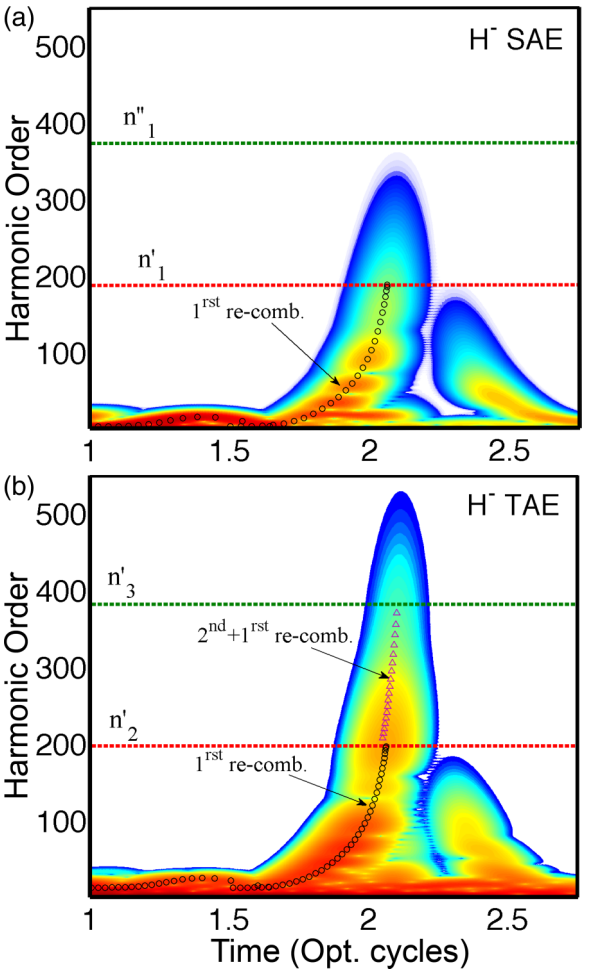

FIG. 5. Gabor transform and semiclassical analysis of the HHG driven by inhomogeneous fields for (a) the SAE and (b) the TAE models of H^-. The color scale is logarithmic and in arbitrary units. Black circles depict the "classical" harmonic emission times considering only the first electron recombination event driven by the inhomogeneous field. In (b) the violet triangles are the emitted harmonics by classically considering the first and the second double nonsequential two-electron recombination events. In (a) the red and green horizontal dashed lines denote the cutoff n_1' and a modification of n_1' which takes into account the first and second recombination (n_1'') for the SAE model. In the case of (b) the TAE model, the same horizontal lines depict the cutoffs denoted by the n_2' and n_3' formulas (see the text).

results of the HHG spectra for both the conventional and spatially inhomogeneous fields are depicted in Figs. 4(a) and 4(b), respectively. Clearly, we observe that both the SAE and TAE are in perfect agreement for the two cases. Slightly reasonable discrepancies are found for low-order harmonics, a region where the details of the atomic potential are relevant. In addition, both the SAE and TAE models' cutoffs are identical, and as a consequence we argue that the outer electron is mainly responsible for the HHG emission process in the case of He. Note that an electric field strength scan of $\mathcal{E}_0 = 0.0535$–0.16 a.u. (1×10^{14}–9×10^{14} W/cm^2) in the calculation of the HHG spectra has been performed for different values of ϵ. The same degree of agreement between the SAE and TAE results was found. It is remarkable that neither an extra extension n_{shift} nor an underestimation on the n_3' cutoff is observed for spatially inhomogeneous fields in the TAE model of He. If we think that the only difference between He and H^- atoms is the nuclear charge, $Z = 2$ for He and $Z = 1$ for H^-, we could infer that not only we should consider how the two electrons dynamics is influenced by the spatial inhomogeneity of the laser electric field, but also what is the role of the Coulomb interaction between the nucleus and each of the electrons.

We can then conclude that single- and double-electron processes play an important role in the description of the emitted HHG from $2e$ systems driven by both conventional and inhomogeneous fields. The latter provides an instrumental tool in order to enhance two-electron effects in certain systems.

B. Time-energy harmonic and classical analysis

In order to further clarify the reasons of the extended HHG spectra for the H^-, we perform a time-energy analysis of the quantum mechanical results in terms of the Gabor transform and a comparison with pure classical simulations [34,35].

Figure 5 depicts the Gabor transform obtained from the quantum mechanically computed HHG spectra of the H^- system driven by a spatially inhomogeneous field for both the SAE [Fig. 5(a)] and TAE [Fig. 5(b)] models, respectively. The

emitted harmonics calculated by the first and second classical recollision electron trajectories are also shown. Excellent agreement between the Gabor synthesis and the classical calculations is found in the case of the SAE picture. Note that only the first recollision event is considered in the classical calculations shown in Fig. 5(a). However, when the TAE approach is employed, the first electron recollision events are not sufficient to reproduce the whole energy range of emitted harmonics described by the Gabor time-frequency decomposition. Nevertheless, if one considers a second recollision event in the classical approach, the maximum harmonic emission is then perfectly reproduced [Fig. 5(b)].

These observations suggest that the main mechanism behind the HHG spectra emitted from our two-electron H^- model driven by a spatially inhomogeneous field can be summarized as follows: (i) The outer electron is ionized via tunneling about one of the maxima of the IR laser pulse. After a while, around the second consecutive maxima, the inner electron is liberated. (ii) The outer electron has a high probability to make a second recollision event together with the first recollision of the inner electron and *both* at the *same* recombination time. As it is established by the n_3' value, the emitted photon energy at this particular time will be the sum of the first and second recombination energies of the two electrons with their respective ground states. This picture is in perfect agreement with the Gabor time-analysis results, extracted from the quantum mechanical models. Furthermore, we can conclude that the main responsibility of the probability increase of this peculiar mechanism is the spatially inhomogeneous character of the plasmonic electric field.

Additionally, the Gabor transform of Fig. 5(a) helps us to disentangle if either the inner and outer electrons are recombining with the remaining ion core at the same recollision time, or if it is only a first and second recombination of a single electron. As it is clearly shown, there is not an emitted harmonic signal at $n_1'' = (E_{\max}^{(1st)} + E_{\max}^{(2nd)} + I_p^{(o)})/\omega_0$. Thereby, it is not possible that the cutoff extension in the HHG spectra obtained from the TAE model comes from a single-electron ionization event followed by a first and second recombination event of this unique electron.

Single- and double-electron ionization probabilities as a function of time provide an estimation of how significant are these channels for each atomic target, namely, H^- and He, during the dynamical laser-atom evolution [18]. Consequently, a comparison of those quantities indicates in which of the studied systems the double ionization is more important. Figure 6 depicts the results. Both, the single and the double-electron ionization probabilities as a function of time are compared for H^- and He, respectively. In case of the hydrogen negative ion we clearly observe that single and double ionization yields quickly increase and reach larger values compared with those of the He atom. In particular, the double-electron ionization yield of He is several orders of magnitude smaller. As the double-electron ground state ionization potential of the hydrogen negative ion is smaller than the helium one, this behavior is obviously expected. For this reason, right after the first laser-cycle, the ratio of double to single ionization for H^- is several orders of magnitude larger than the one for the He atom. As the HHG spectrum depends strongly on the ionization probability [6,19], we can

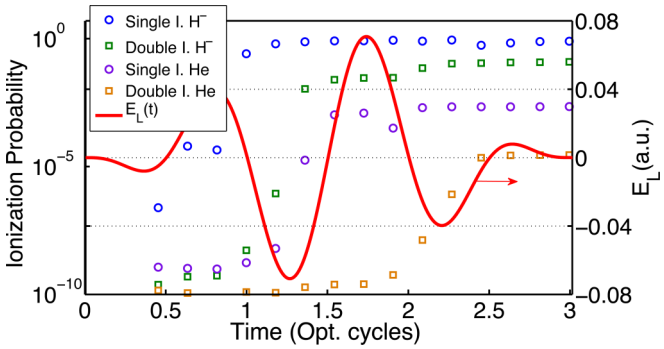

FIG. 6. Single and double electron ionization probabilities for the H^- and He model atoms. Blue (violet) circles and green (orange) squares depict the single and double electron ionization yields as a function of time for the hydrogen negative ion (helium) atom, respectively. The laser electric field is shown in the red solid line. The parameters used are the same as in Fig. 2 and the spatially inhomogeneous field parameter is $\epsilon = 0.02$ a.u.

then expect that the NSDR process might be more likely in H^- than in He.

The fact that the double electron ionization channel is larger in the case of H^- compared with He, does not exactly mean that the double recombination process will be enhanced as well. A full analytical answer to this question is difficult due to the complexity of the relationships between the electron-electron correlation and the electron-nucleus interactions, both of Coulombic character, combined with the spatial inhomogeneity of the laser electric field.

We could give, nevertheless, some light about the role of the spatially inhomogeneous field in the NSDR process by performing a semiclassical calculation solving the Newton equation of motion of an electron moving in the electric field of the laser. We compute classical trajectories such as those they can recollide with the ion core several times for both scenarios, namely, the homogeneous and inhomogeneous fields. Figures 7(a) and 7(b) show these results, respectively. It is clear that the spatially inhomogeneous field refocuses higher energetic electron trajectories towards the ion core, thus allowing the double electron recollision process with electrons with larger kinetic energies [see dashed lines in Fig. 7(b)]. This fact added to the large double-electron ionization probability clearly support our hypothesis that a NSDR mechanism takes place in the HHG process in the case of H^- (for the case of He this process is also possible, but due to the small probability of the double ionization channel, the chances to observe it in the HHG spectrum are negligible).

Additional questions about the roles of both the *e-e* repulsion and the Coulomb interaction of each of the electrons with the nucleus can naturally appear, which we are unable to answer with only a semiclassical approach. For the former we have performed additional simulations turning off the *e-e* correlation term for the case of H^- driven by a spatially inhomogeneous field (for He we have seen there is no difference between the SAE and the TAE simulations). Our calculations support the fact that without considering the *e-e* correlation, such a big extension in the HHG cutoff observed in Fig. 2(b) will not be possible.

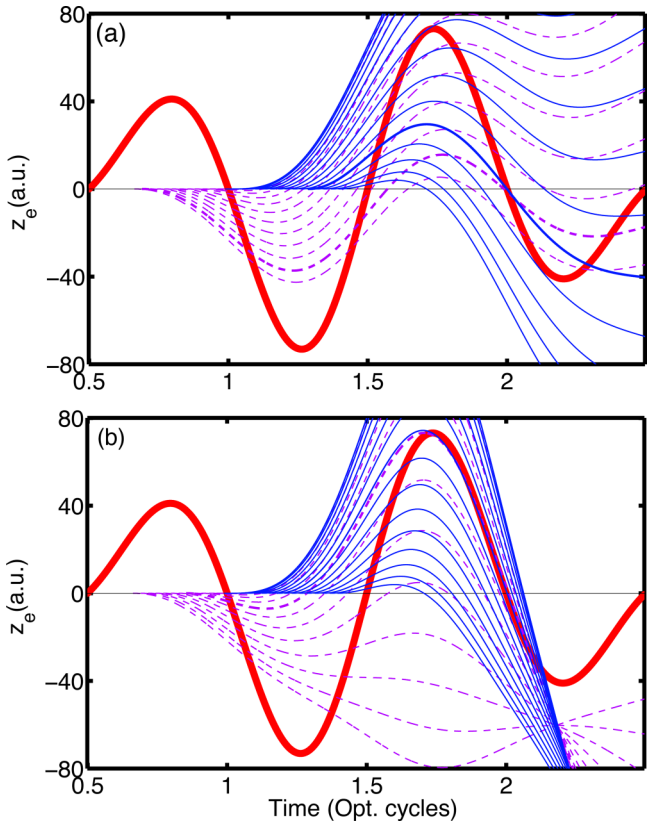

FIG. 7. Classical electron trajectories obtained by using the Newton equation of motion for both the spatially homogenous (a) $\epsilon = 0.0$ a.u. and inhomogeneous (b) $\epsilon = 0.02$ a.u. fields, respectively. The set of violet (dashed) lines denotes possible electron trajectories with double recollision with the atomic nucleus. The set of the blue (solid) ones are those trajectories which have only one recollision event with the remaining ion core. Red thick lines in both panels represent the time dependence of the IR electric field $E_h(t)$. The other laser parameters are the same as those used in Fig. 2.

For the latter, i.e., about the role of the Coulomb electron-nucleus interaction, we can only speculate that it takes part in the process, analyzing the differences between the HHG spectra of He and H^- computed by both the SAE and TAE (see the previous section). This asseveration is not, however, in contradiction with the conclusions of Ref. [19], where the authors claim the *e-e* correlation is one of the main responsible of the NSDR. We could argue that this is due to the fact that they have analyzed only the He case and for other species the situation could substantially change.

Hence, we have collected convincing arguments, based both on quantum mechanical and classical analysis, that a mechanism, dubbed NSDR, is mainly responsible for the extension of the HHG spectra of the H^- when a spatially inhomogeneous plasmonic field is used to drive the process.

IV. CONCLUSIONS

Summarizing, we have performed two-electron calculations of HHG driven by spatially homogeneous and inhomogeneous fields. We used as test systems H^- and He. By the numerical solution of 1D-TDSE models in the single- and two-active electron approximations, supported by a classical analysis of the electron trajectories, we have demonstrated that an extra extension in the harmonic cutoff was found in case of the TAE model for H^-, which cannot be explained within the SAE framework. After a comprehensive analysis using complementary tools, we have concluded that NSDR is mainly responsible for this extension. One of the main advantages to using plasmonic fields as "probes" is the low incoming intensity needed in order to observe this effect, considering that the plasmonic nanostructures act as light amplifiers. In addition, as we have shown, the results strongly depend on the atomic system employed. In particular, the H^- was chosen for simplicity, but we consider similar effects and results could be found for highly correlated negative ion systems, such as the alkali negative ions [36]. In order to find the correct target to experimentally observe these mechanisms, reliable calculations of double to single ionization ratios would be instrumental.

ACKNOWLEDGMENTS

A.C. and M.L. acknowledge the Spanish MINECO (FIS2013-46768-P FOQUS and Severo Ochoa SEV-2015-0522), the AGAUR Grant No. 2014 SGR 874, the Fundació Cellex Barcelona, and the ERC AdG OSYRIS. We also acknowledge the support from the EC's Seventh Framework Programme LASERLAB-EUROPE III (Grant Agreement No. 284464) and the Ministerio de Economía y Competitividad of Spain (FURIAM Project FIS2013-47741-R). M.F.C. was supported by the project ELI-Extreme Light Infrastructure-Phase 2 (CZ.02.1.01/0.0/0.0/15 008/0000162) from the European Regional Development Fund. The authors thankfully acknowledge the computer resources, technical expertise, and assistance provided by the Red Española de Supercomputación. We also thanks F. Cucchietti for useful comments and support.

[1] M. Nisoli, S. D. Silvestri, O. Svelto, R. Szipöcs, K. Ferencz, C. Spielmann, S. Sartania, and F. Krausz, Opt. Lett. **22**, 522 (1997).
[2] A. L'Huillier and P. Balcou, Phys. Rev. Lett. **70**, 774 (1993).
[3] F. Krausz and M. Ivanov, Rev. Mod. Phys. **81**, 163 (2009).
[4] M. Ferray, A. L'Huillier, X. F. Li, L. A. Lompre, G. Mainfray, and C. Manus, J. Phys. B **21**, L31 (1988).
[5] P. B. Corkum, Phys. Rev. Lett. **71**, 1994 (1993).
[6] M. Lewenstein, P. Balcou, M. Yu. Ivanov, A. L'Huillier, and P. B. Corkum, Phys. Rev. A **49**, 2117 (1994).
[7] S. Kim, J. Jin, Y.-J. Kim, I.-Y. Park, Y. Kim, and S.-W. Kim, Nature (London) **453**, 757 (2008).
[8] M. Sivis, M. Duwe, B. Abel, and C. Ropers, Nature (London) **485**, E1 (2012).
[9] S. Kim, J. Jin, Y.-J. Kim, I.-Y. Park, Y. Kim, and S.-W. Kim, Nature (London) **485**, E1 (2012).

[10] M. Sivis, M. Duwe, B. Abel, and C. Ropers, Nat. Phys. **9**, 304 (2013).
[11] T. Shaaran, M. F. Ciappina, and M. Lewenstein, J. Mod. Opt. **59**, 1634 (2012).
[12] A. Husakou, S.-J. Im, and J. Herrmann, Phys. Rev. A **83**, 043839 (2011).
[13] M. F. Ciappina, J. Biegert, R. Quidant, and M. Lewenstein, Phys. Rev. A **85**, 033828 (2012).
[14] I. Yavuz, E. A. Bleda, Z. Altun, and T. Topcu, Phys. Rev. A **85**, 013416 (2012).
[15] M. F. Ciappina, S. S. Aćimović, T. Shaaran, J. Biegert, R. Quidant, and M. Lewenstein, Opt. Exp. **20**, 26261 (2012).
[16] J. A. Pérez-Hernández, M. F. Ciappina, M. Lewenstein, L. Roso, and A. Zaïr, Phys. Rev. Lett. **110**, 053001 (2013).
[17] D. G. Lappas, A. Sanpera, J. B. Watson, K. Burnett, P. L. Knight, R. Grobe, and J. H. Eberly, J. Phys. B **29**, L619 (1996).
[18] R. Grobe and J. H. Eberly, Phys. Rev. A **48**, 4664 (1993).
[19] P. Koval, F. Wilken, D. Bauer, and C. H. Keitel, Phys. Rev. Lett. **98**, 043904 (2007).
[20] A. D. Bandrauk and H.-Z. Lu, J. Phys. B **38**, 2529 (2005).
[21] H. Shi-Lin and S. Ting-Yun, Chin. Phys. B **22**, 013101 (2013).
[22] R. Santra and A. Gordon, Phys. Rev. Lett. **96**, 073906 (2006).
[23] J. Prager, S. X. Hu, and C. H. Keitel, Phys. Rev. A **64**, 045402 (2001).
[24] M. Protopapas, C. H. Keitel, and P. L. Knight, Rep. Prog. Phys. **60**, 389 (1997).
[25] M. F. Ciappina, J. A. Pérez-Hernández, T. Shaaran, J. Biegert, R. Quidant, and M. Lewenstein, Phys. Rev. A **86**, 023413 (2012).
[26] M. Lein, E. K. U. Gross, and V. Engel, Phys. Rev. Lett. **85**, 4707 (2000).
[27] G. Pöschl and E. Teller, Z. Phys. **83**, 143 (1933).
[28] A. Chacón, M. F. Ciappina, and A. P. Conde, Eur. Phys. J. D **69**, 133 (2015).
[29] R. Grobe and J. H. Eberly, Phys. Rev. A **47**, R1605 (1993).
[30] M. D. Feit, J. A. Fleck, and A. Steiger, J. Comput. Phys. **47**, 412 (1982).
[31] M. Frigo and S. G. Johnson, FFTW library (1998), http://www.fftw.org
[32] C. Ruiz and A. Chacón, QFISHBOWL library (2008), http://code.google.com/p/qfishbowl
[33] J. B. Watson, A. Sanpera, D. G. Lappas, P. L. Knight, and K. Burnett, Phys. Rev. Lett. **78**, 1884 (1997).
[34] D. Gabor, J. Inst. Electr. Eng. **93**, 429 (1946).
[35] C. C. Chirila, I. Dreissigacker, E. V. van der Zwan, and M. Lein, Phys. Rev. A **81**, 033412 (2010).
[36] E. Clementi and A. D. McLean, Phys. Rev. **133**, A419 (1964).